

Intraoperative Application of Optical Spectroscopy in the Presence of Blood

Wei-Chiang Lin, Steven A. Toms, E. Duco Jansen, and Anita Mahadevan-Jansen

Abstract—A simple but effective method of spectral processing was developed to minimize or remove the effects of the presence of superficial blood on tissue optical spectra and, hence, enhance the performance of optical-spectroscopic-based *in vivo* tissue diagnosis and surgical guidance. This spectral-processing algorithm was developed using the principles of absorption-induced light attenuation wherein the ratio of fluorescence intensity (F) and the h th power of diffuse reflectance intensity (Rd) at a given emission wavelength λ_m is immune to spectral distortions induced by the presence of blood on the tissue surface. Here, the exponent h is determined by the absorption coefficients of whole blood at the excitation and emission wavelengths. The theoretical basis of this spectral processing was verified using simulations and was experimentally validated. Furthermore, the optical spectra of brain tissues collected *in vivo* was processed using this algorithm to evaluate its impact on brain tissue differentiation using combined fluorescence and diffuse reflectance spectroscopy. Based on the simulation, as well as experimental results, it was observed that using F/Rd^h can effectively reduce or remove spectral distortions induced by superficial blood contamination on tissue optical spectra. Thus, optical spectroscopy can also be used intraoperatively for applications such as surgical guidance of tumor resection.

Index Terms—Deoxyhemoglobin, diffuse reflectance spectroscopy, fluorescence spectroscopy, optical diagnosis, oxy-hemoglobin, spectral attenuation, surgical guidance.

I. INTRODUCTION

TISSUE diagnosis using optical spectroscopy, also known as optical biopsy, has been extensively studied for many organ sites over the past decade [1], [2]. The attraction of this modality arises primarily from the fact that optical spectroscopy is capable of noninvasively investigating the physiological and morphological characteristics of tissue in real or near real-time. To date, the validity and effectiveness of tissue diagnosis using optical spectroscopy have been demonstrated in many tissue organs *in vivo* [1], [2]. Fluorescence spectroscopy alone has often been utilized for tissue discrimination in these studies as it provides adequate signal strength and contains a wealth of diagnostic information [1]. Interpretation of tissue fluorescence spectra, however, is rather difficult; fluorescence spectra measured from bulk tissues can be significantly different from those

from pure tissue fluorophores due to the interplay of tissue optics. It has been hypothesized that removing the effect of tissue optical properties could facilitate tissue diagnosis using fluorescence spectroscopy alone [3]–[8]. In other words, an intrinsic fluorescence spectrum (without distortions induced by absorption and scattering) should be more useful than a raw tissue fluorescence spectrum in optical diagnosis. Based on this idea, a variety of models have been developed for retrieving an intrinsic fluorescence spectrum from a measured fluorescence spectrum [3]–[8]. Despite the differences in their theoretical bases, all these models utilize diffuse reflectance spectroscopy to recover the intrinsic fluorescence spectra from the measured fluorescence spectra assuming a homogenous, one-dimensional, highly scattering medium. These models, however, cannot be applied to media with high absorption coefficients or consisting of multiple layers. In addition, the optical characteristics of tissue—removed during the recovery of intrinsic fluorescence—may possess useful diagnostic information. For example, it is known that blood absorption signatures are more pronounced in tumor tissues due to high blood content [9]–[11]. More importantly, the advantages of using intrinsic tissue fluorescence for *in vivo* tissue diagnosis have yet to be thoroughly evaluated.

Optical spectroscopy has been recently developed as a feedback tool for intraoperative guidance of surgeries [12]–[16]. For example, we are currently investigating the use of combined fluorescence and diffuse reflectance spectroscopy for *in vivo* brain tumor demarcation and preliminary results have been promising [16]. However, a major challenge arises from implementing optical spectroscopy for surgical guidance: the inevitable presence of residual blood at the surface of the site under investigation (i.e., superficial blood contamination) that degrades the accuracy of tissue discrimination using optical spectroscopy. It has been previously observed [16] that the inefficiency of fluorescence spectroscopy in separating normal brain tissues from brain tumors *in vivo* is primarily attributed to the inherent bloody nature of the operating field. To successfully use optical spectroscopy for intraoperative guidance of brain tumor resection, the effect of this superficial blood contamination has to be minimized or eliminated. Thus, a series of theoretical and experimental studies were performed to investigate the effect of superficial blood contamination on tissue optical spectra, and to develop a discrimination parameter (based on fluorescence, reflectance or a combination thereof) that accounts for this effect.

In this study, we present a simple but novel model wherein, rather than extracting the intrinsic tissue fluorescence, the measured tissue fluorescence and diffuse reflectance spectra are uniquely combined such that the attenuation effect of superficial blood contamination can be minimized or removed completely.

Manuscript received May 22, 2001; revised October 22, 2001.

W.-C. Lin, E. D. Jansen, and A. Mahadevan-Jansen are with the Department of Biomedical Engineering, Vanderbilt University, Nashville, Tennessee 37235 USA (e-mail: linw@vuse.vanderbilt.edu).

S. A. Toms was with the Department of Neurological Surgery, Vanderbilt University Medical Center, Nashville, TN 37235 USA. He is now with Oregon Health Sciences University, Portland, OR 97201 USA.

E. D. Jansen and A. Mahadevan-Jansen are with the Department of Neurological Surgery, Vanderbilt University Medical Center, Nashville, TN 37235 USA.

Publisher Item Identifier S 1077-260X(01)11194-9.

This theoretical model was established to analyze the attenuation effect of blood contamination on tissue fluorescence and diffuse reflectance spectra, which uncovered a combined spectrum independent from superficial blood contamination. The theory was then validated using Monte Carlo simulations and an experimental study. To further validate the utility of this rather simple model and its effect on tissue discrimination, the model was applied to *in vivo* tissue spectra obtained from two brain tumor patients (a subset of an ongoing clinical brain tumor study). Discrimination algorithms were developed using the raw spectral data, as well as those processed with the new model separately, and their performances were compared.

II. THEORY

Between 300 and 600 nm, the primary effect of superficial blood contamination on tissue optical spectra is absorption, i.e., additional attenuation is introduced to both the excitation and the emission light. Assuming that the layer of blood at the tissue surface is physically thin (i.e., less than 100 μm) and homogeneous, the percentage of light transmitted through this blood layer A [%] can be described using Beer's law as $A = \exp[-\mu_a(\lambda) \times d] \times 100\%$, where $\mu_a(\lambda)$ [cm^{-1}] is the wavelength-dependent absorption coefficient of blood and d [cm] is the thickness of the blood layer. In this paper, the exponent $\mu_a(\lambda) \times d$ in Beer's law is denoted as the attenuation coefficient α . The fluorescence signal $F_c(\lambda_m)$ measured from a blood contaminated tissue sample, therefore, can be written as

$$\begin{aligned} F_c(\lambda_m) &= F_o(\lambda_m) \times \exp[-\mu_a(\lambda_x) \times d] \\ &\quad \times \exp[-\mu_a(\lambda_m) \times d] \\ &= F_o(\lambda_m) \times \exp[-(k+1) \times \mu_a(\lambda_m) \times d] \\ &= F_o(\lambda_m) \times \exp(-\alpha_f) \end{aligned} \quad (1)$$

where

λ_m	emission wavelength;
λ_x	excitation wavelength;
$F_o(\lambda_m)$	fluorescence intensity at λ_m from tissue without blood contamination;
k	$= \mu_a(\lambda_x) / \mu_a(\lambda_m)$
α_f	fluorescence attenuation coefficient.

The same principle can also be applied to the contaminated diffuse reflectance signal $Rd_c(\lambda_m)$. That is

$$\begin{aligned} Rd_c(\lambda_m) &= Rd_o(\lambda_m) \times \exp[-\mu_a(\lambda_m) \times d] \\ &\quad \times \exp[-\mu_a(\lambda_m) \times d] \\ &= Rd_o(\lambda_m) \times \exp[-2 \times \mu_a(\lambda_m) \times d] \\ &= Rd_o(\lambda_m) \times \exp(-\alpha_{Rd}) \end{aligned} \quad (2)$$

where $Rd_o(\lambda_m)$ is the diffuse reflectance at λ_m from tissue without blood contamination and α_{Rd} is the diffuse reflectance attenuation coefficient.

The exponential terms in (1) and (2) can be eliminated by taking the ratio of $F_c(\lambda_m)$ and the h th power of $Rd_c(\lambda_m)$. As a result

$$\frac{F_c(\lambda_m)}{Rd_c(\lambda_m)^h} = \frac{F_o(\lambda_m)}{Rd_o(\lambda_m)^{(k+1)/2}} \quad (3)$$

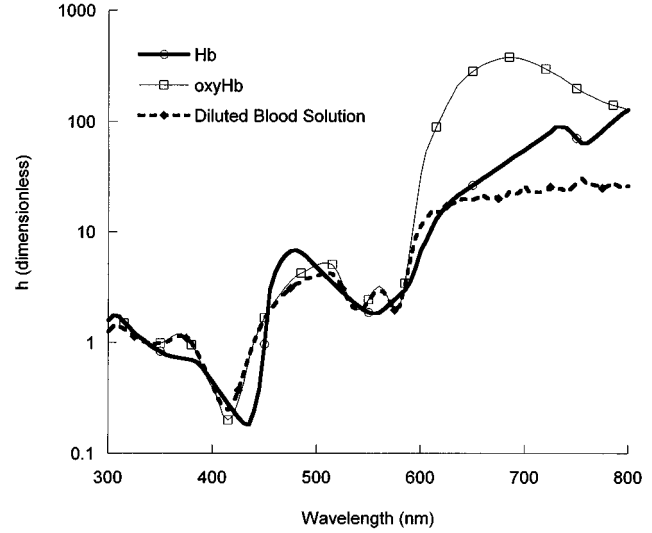


Fig. 1. Exponents $h(\lambda)$ for hemoglobin, oxyhemoglobin, and diluted blood solution between 300- and 800-nm emission calculated using 337-nm excitation.

where the exponent $h = (k+1)/2$. Note that the new combined spectrum F/Rd^h is not affected by the degree of superficial blood contamination.

Since hemoglobin is the primary chromophore in blood in the spectral region of interest (i.e., 300–600 nm) and the partial pressure of oxygen in air is about 150 mmHg, the absorption coefficients of blood ($\mu_{a,\text{blood}}(\lambda)$) present at the tissue surface should be very similar to that of a solution of oxyhemoglobin (oxyHb) with a concentration of 150 g/L ($\mu_{a,\text{oxyHb}}(\lambda)$) [17]. Based on this assumption, k and h were found to be 2.38 and 1.69, respectively, when, for example, $\lambda_x = 337$ nm ($\mu_{a,\text{oxyHb}} = 549$ cm^{-1}) and $\lambda_m = 460$ nm ($\mu_{a,\text{oxyHb}} = 231$ cm^{-1}) [17]. In other words, the theory predicts that, e.g., taking $F/Rd^{1.69}$ at 337-nm excitation, 460-nm emission should eliminate (or minimize) the effect of superficial blood contamination. The exponents $h(\lambda)$ can be calculated for other emission wavelengths using the same method (see Fig. 1).

III. MATERIALS AND METHODS

To test the validity of the theory described above, a series of simulations and experimental studies were conducted. In addition, the theory was applied to two sets of optical spectra obtained clinically from brain tumor patients *in vivo* to prove its effectiveness in improving tissue discrimination.

A. Monte Carlo Simulation

A two-layer Monte Carlo fluorescence simulation model was built in accordance to the principles described by Welch and van Gemert [18] to validate the theory derived in Section II. A brief description of this Monte Carlo model is provided here. The incident, or in this case excitation photons, are launched into a tissue phantom in a direction normal to the surface, and then propagated based on the optical properties of the tissue phantom. After propagating a single step, a portion of the excitation photon energy ΔE is deposited into the local tissue, which

TABLE I
ESSENTIAL PARAMETERS OF THE TISSUE PHANTOMS USED IN THE MONTE CARLO SIMULATIONS

Layer	Optical Properties				n [#]	Fluorescence Efficiency	Thickness d [cm]
	$\mu_a(337 \text{ nm})$ [cm ⁻¹]	$\mu_s'(337 \text{ nm})^*$ [cm ⁻¹]	$\mu_a(460 \text{ nm})$ [cm ⁻¹]	$\mu_s'(460 \text{ nm})$ [cm ⁻¹]		Q	
1	$545 \times B^{\S}$, B = 0 ~ 90%	0	$231 \times B$, B = 0 ~ 90%	0	1.4	0	0.01
2	4.72	76.7	2	67.2	1.4	0.01	5

* μ_s' is the reduced scattering coefficient

n is the index of refraction

§ B is the blood content [%] increasing from 0 to 90% at a interval of 10%

results in the emission of a fluorescence photon in a random direction. The initial energy of the fluorescence photon is determined by the product of ΔE and the quantum yield Q of the tissue fluorophore. The newly-generated fluorescence photon is then propagated in the tissue phantom using the same rules as those for the excitation photons. At the end of each simulation, the model produces a distribution of reflected excitation photons Rd and remitted fluorescence photons F as a function of radial position r [cm] and escape angle θ (degree). The same model was also used to simulate diffuse reflectance by assigning the quantum yield of tissue fluorophore to zero. To reduce the complexity of the simulation model, only one excitation and emission wavelength were considered in a single run of the simulation; the excitation wavelength was maintained at 337 nm and the emission wavelength at 460 nm in all simulations.

The tissue geometry utilized in the simulations was assumed to be homogenous, semi-infinite media consisting of two optically distinct layers; a 100- μm -thick absorbing medium at the top, simulating surface blood, and a 5-cm-thick layer below, simulating the biological tissue (i.e., white matter, in this case). The optical properties of each layer are listed in Table I. Note that the reduced scattering coefficient of the top absorbing layer was assigned to zero, as the anisotropy factor of blood is very close to one [19]. Optical properties of brain white matter were measured using a spectrophotometer with an integrating sphere module and the inverse adding-doubling model [20]. To emulate the collection geometry of the fiberoptic probe used in the experimental study described in Section III-B, a collimated excitation beam with a uniform beam profile and a beam diameter of 300 μm was used in each simulation. In addition, the values of F_{460} and Rd_{460} measured from each tissue phantom were calculated by integrating the remitted fluorescence photons $F(r, \theta)$ and reflected $Rd(r, \theta)$ excitation photons, respectively, from $r = 150$ to 450 μm and $\theta = 0^\circ$ to 30° . Overall, ten simulations with varying degrees of blood contamination were performed (Table I). The number of photons used in each simulation was equal to or greater than 500 000 to ensure a good statistical accuracy of the simulation results.

B. Experimental Study

To experimentally validate the theory proposed in this paper, fluorescence and diffuse reflectance spectra were measured from chicken breast samples *in vitro* with varying degrees of

blood contamination. F/Rd^h was calculated at several emission wavelengths and compared within and between samples. Chicken breast muscle tissue was used in this study as it displays fluorescence between 400 and 600 nm and its structure is relatively homogenous over a large area. Human blood drawn from a volunteer was diluted using phosphate buffered saline (PBS) and applied to the tissue surface to emulate superficial blood contamination in the operating field. A fiberoptic based spectrometer was used to acquire fluorescence and diffuse reflectance spectra from the tissue samples. The spectroscopic system contains two excitation light sources: a nitrogen laser (337-nm, 20-ns laser pulse-width, 10 $\mu\text{J}/\text{pulse}$ at tissue surface, 20-Hz repetition rate) for fluorescence measurements and a broadband halogen light (2 mW at tissue surface) for diffuse reflectance measurements. The excitation light was delivered to the investigated site using a fiberoptic probe. The remitted light, (fluorescence and diffuse reflectance) was collected by the same probe, transmitted to a spectrograph, and then dispersed onto a CCD camera. To achieve adequate spectral signal to noise ratio, an integration time of 2 s was used for each spectral measurement. Three spectra, background, fluorescence, and diffuse reflectance, were sequentially acquired from the tissue sample during each investigation. The absorption spectrum of the diluted blood solution was measured at the end of the study using a spectrophotometer¹ and the absorption coefficients $\mu_{a,\text{diluted_blood}}(\lambda)$ were then used to calculate the values of the exponent $h(\lambda)$ of dilute blood.¹

Prior to the application of diluted blood, blood-contamination-free fluorescence and diffuse reflectance spectra, $F_o(\lambda)$ and $Rd_o(\lambda)$, were measured from the tissue sample. A drop of diluted blood was then applied to the surface of the sample, and another set of fluorescence and diffuse reflectance spectra, $F_c(\lambda)$ and $Rd_c(\lambda)$, were recorded. Each sample was used only once, as the diluted blood solution penetrated into the tissue and could not be completely removed. The optical probe was lightly placed in contact with the tissue surface during spectral acquisition to avoid excessive compression of the tissue.

Prior to the F/Rd^h calculation, all acquired optical spectra were preprocessed to account for background signal and spectral variations introduced by the spectrometer [16]. The attenuation coefficients at various emission wavelengths $\alpha_f(\lambda_m)$, which reflect the degree of blood contamination,

¹Lambda 900, Perkin Elmer.

were calculated using $F_c(\lambda_m)/F_o(\lambda_m)$ and (2). Finally, $(F_c/Rd_c^h)/(F_o/Rd_o^h)$ at various emission wavelengths were calculated for each sample using the values of $h(\lambda)$ previously determined from the diluted blood measurements.

C. Clinical Data Analysis

In order to understand the influence of the new model on *in vivo* brain tissue discrimination, $F/Rd^h(\lambda)$ were calculated using the *in vivo* spectra acquired from brain tumor patients and utilized to develop discrimination algorithms. The protocol used for the acquisition of the clinical spectra is described elsewhere [16]. Two sets of clinical data from two human patients were used for this evaluation: one with a strong degree of superficial blood contamination and the other with a weak degree of superficial blood contamination. The calibrated fluorescence spectra and their corresponding diffuse reflectance spectra from these two clinical data sets were combined to calculate $F/Rd^h(\lambda)$ between 400 and 600 nm for the investigated brain tissue sites. Empirical discrimination algorithms were developed based on F/Rd^h with respect to Rd and F with respect to Rd . The optimal performances of the discrimination algorithms were compared to evaluate the capability of the F/Rd^h model in separating the different tissue types regardless of the degree of superficial blood contamination.

IV. RESULTS

The exponents $h(\lambda)$ of diluted blood, oxyhemoglobin, and hemoglobin ($h_{\text{dilute_blood}}$, h_{oxyHb} , and h_{Hb}) between 300 and 800 nm are shown in Fig. 1. Clearly, the line shape of $h_{\text{dilute_blood}}$ is almost identical to h_{oxyHb} between 300 and 600 nm, although small differences in their amplitudes can be seen at 415 and 500 nm. Nevertheless, the similarity between $h_{\text{dilute_blood}}$ and h_{oxyHb} supports a critical hypothesis proposed in the theoretical development: the absorption characteristics of blood contamination between 300 and 600 nm can be solely characterized by oxyhemoglobin absorption.

The results of the simulation study, shown in Fig. 2, prove that F/Rd^h is not subject to spectral attenuation due to the presence of superficial blood contamination. The simulated curve of F_c/F_o at 460-nm emission in Fig. 2 indicates that the collected fluorescence emission decreases exponentially as the degree of superficial blood contamination (as indicated by α_f) increases, which concurs with the prediction of (1). The ratio of $F(460 \text{ nm})$ and $Rd(460 \text{ nm})$ also shows an exponential decay as a function of α_f ; although the decrease rate of $F(460 \text{ nm})/Rd(460 \text{ nm})$ is lower than that of $F(460 \text{ nm})$ alone. This suggests that the direct ratio of fluorescence and diffuse reflectance can reduce, but not completely remove, the effect of superficial blood contamination. Furthermore, the simulation shows that the degree of blood contamination has no effect on $F(460 \text{ nm})/Rd(460 \text{ nm})^{1.69}$, which is evidenced by the flat line of $F(460 \text{ nm})/Rd(460 \text{ nm})^{1.69}$ over the entire range of α_f examined in the simulation study. This unequivocally supports the theory derived in this paper.

Fig. 3(a)–(c) are the plots of F/Rd^h with respect to α_f at 460-, 500-, and 540-nm emission, respectively, obtained from chicken breast tissues. Three sets of experimental data are pre-

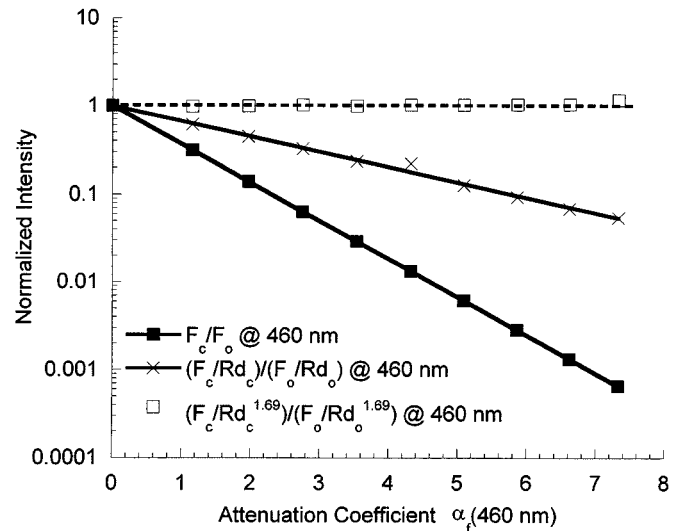


Fig. 2. Normalized F [■], F/Rd [×] and $F/Rd^{1.69}$ [□] at 460-nm emission (337-nm excitation) for different degrees of superficial blood contamination. Solid lines: Curve-fitted lines of F and F/Rd , which reveal their trends. Dashed line: Theoretical prediction of $F/Rd^{1.69}$.

sented in each plot: F_c/F_o , $[F_c/Rd_c^h]/[F_o/Rd_o^h]$ calculated with $h = h_{\text{dilute_blood}}$ and $[F_c/Rd_c^h]/[F_o/Rd_o^h]$ calculated with $h = h_{\text{oxyHb}}$. The distribution of the data points along the α_f axis is fairly even, which indicates that different degrees of superficial blood contamination were achieved in the experimental study. Overall, F/Rd^h showed little or no attenuation due to superficial blood contamination at all emission wavelengths, when α_f was less than 2. Both $h_{\text{dilute_blood}}$ and h_{oxyHb} yielded F/Rd^h values that were insensitive to superficial blood contamination with $\alpha_f < 2$ (i.e., fluorescence attenuation $< 86\%$). This, again, confirms the validity of the assumption regarding the absorption characteristics of blood used in the theory derivation. When α_f exceeded 2, the effect of superficial blood contamination on F/Rd^h becomes significant; the deviation between experimental data and theoretical prediction significantly increases as α_f increases.

The advantage of combining the tissue optical spectra based on the simple F/Rd^h model for *in vivo* brain tissue differentiation is demonstrated in Figs. 4 and 5. These figures represent the optimal discrimination outcomes of the discrimination algorithms based on F versus Rd and F/Rd^h versus Rd . In the case where the degree of superficial blood contamination was insignificant, it was found that fluorescence alone could best separate brain tumor tissues from normal brain tissues [see Fig. 4(a)] with no misclassification at 460-nm emission. The empirical discrimination algorithm based on F/Rd^h ($h = 1.01$), as shown in Fig. 4(b), could best classify all the samples distinctly at $F(440 \text{ nm})$, $Rd(440 \text{ nm})$, and $Rd(625 \text{ nm})$ with better separation distances. In the case where superficial blood contamination was more pronounced, the fluorescence signal alone could no longer provide a clear separation between normal brain and tumor tissues [see Fig. 5(a)]. Using $F(460 \text{ nm})$ in conjunction with $Rd(625 \text{ nm})$, the 2-D discrimination algorithm shown in Fig. 5(a) still misclassified one brain tissue sample. However, the empirical discrimination algorithm based on F/Rd^h ($h = 1.01$) at $F(440 \text{ nm})$ and

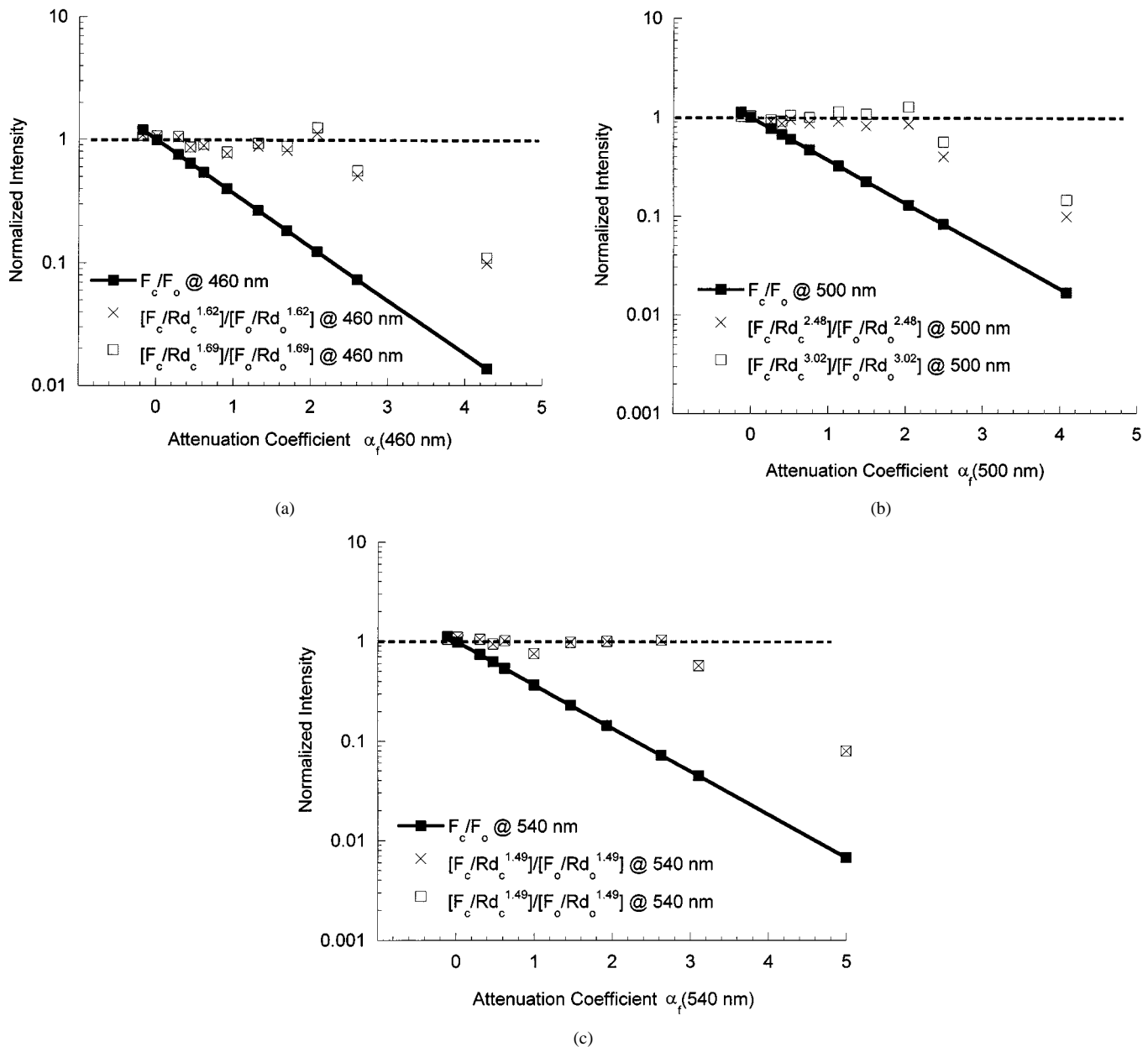


Fig. 3. Normalized F [■], F/Rd^h with $h = h_{\text{diluted_blood}}$ [×] and F/Rd^h with $h = h_{\text{oxyHb}}$ [□] at: (a) 460-, (b) 500-, and (c) 540-nm emission (337-nm excitation) obtained from chicken breast tissue. Solid line: Curve-fitted line for normalized F . Dashed line: Theoretical prediction of F/Rd^h .

$F(625 \text{ nm})$, as shown in Fig. 5(b), could correctly classify all the samples despite the presence of superficial blood contamination.

V. DISCUSSION

Superficial blood contamination of tissue, which is inevitable in a surgical procedure such as tumor resection, hampers the accuracy of optical spectroscopy for intraoperative surgical guidance. To overcome this obstacle, a method of spectral processing was developed using the principle of absorption-induced light attenuation, which generates a new combined spectrum F/Rd^h , free of the attenuation effect of superficial blood contamination. The theoretical basis of the spectral processing algorithm was verified using Monte Carlo simulations as well as in an *in vitro* experimental study. Furthermore, the theory was applied to

two sets of *in vivo* brain tissue spectra with different degrees of superficial blood contamination. The discrimination algorithm utilizing F/Rd^h as one of the differential criteria resulted in a better brain tissue differentiation than the one based on raw spectral data.

Two important assumptions were made in the derivation of the theoretical basis, the F/Rd^h model, of this paper. First, the theory postulates that the blood layer on the tissue surface is physically thin; hence, light attenuation through this blood layer can be described by Beer's Law. This assumption is valid when optical spectra are acquired using a contact fiberoptic probe, as described earlier. However, the validity of this assumption, and hence the F/Rd^h model, in a spectral imaging modality (i.e., noncontact) has yet to be determined. Second, the theory postulates that the exponents $h(\lambda)$ of the blood layer can be directly calculated from the absorption spectrum

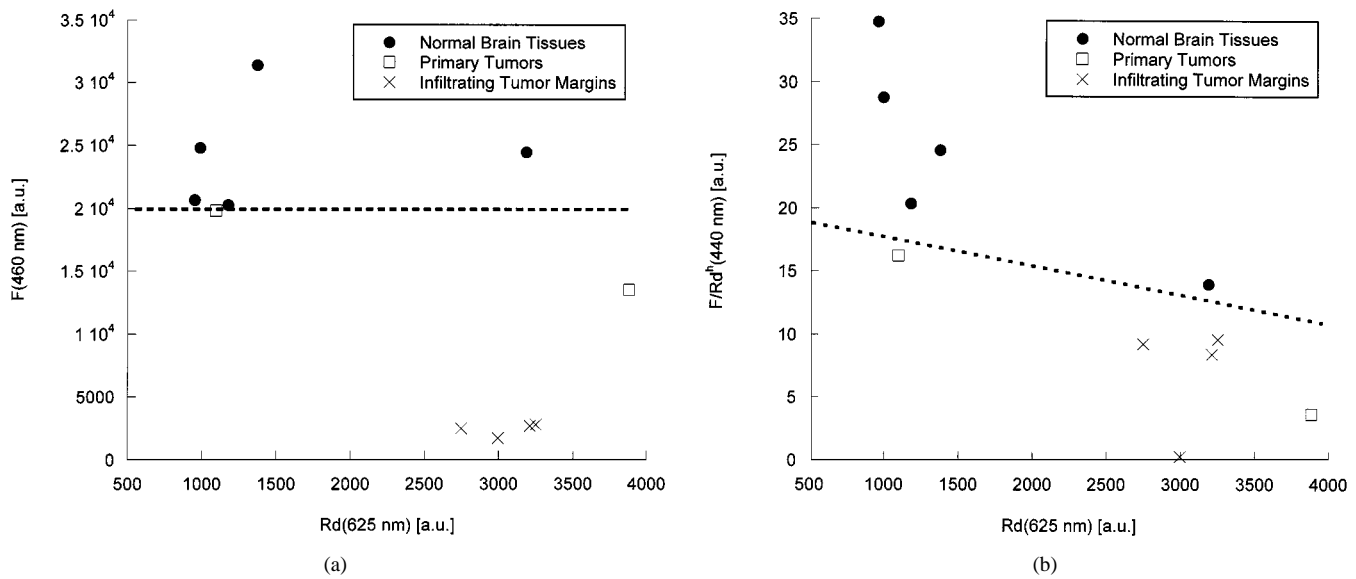


Fig. 4. Empirical discrimination algorithms for *in vivo* brain tissue data set with a low degree of superficial blood contamination based on: (a) $F(460 \text{ nm})$ and $Rd(625 \text{ nm})$ and (b) $F/Rd^{1.01}$ at 440 nm and $Rd(625 \text{ nm})$. Dashed line: Cutoff for brain tissue separation.

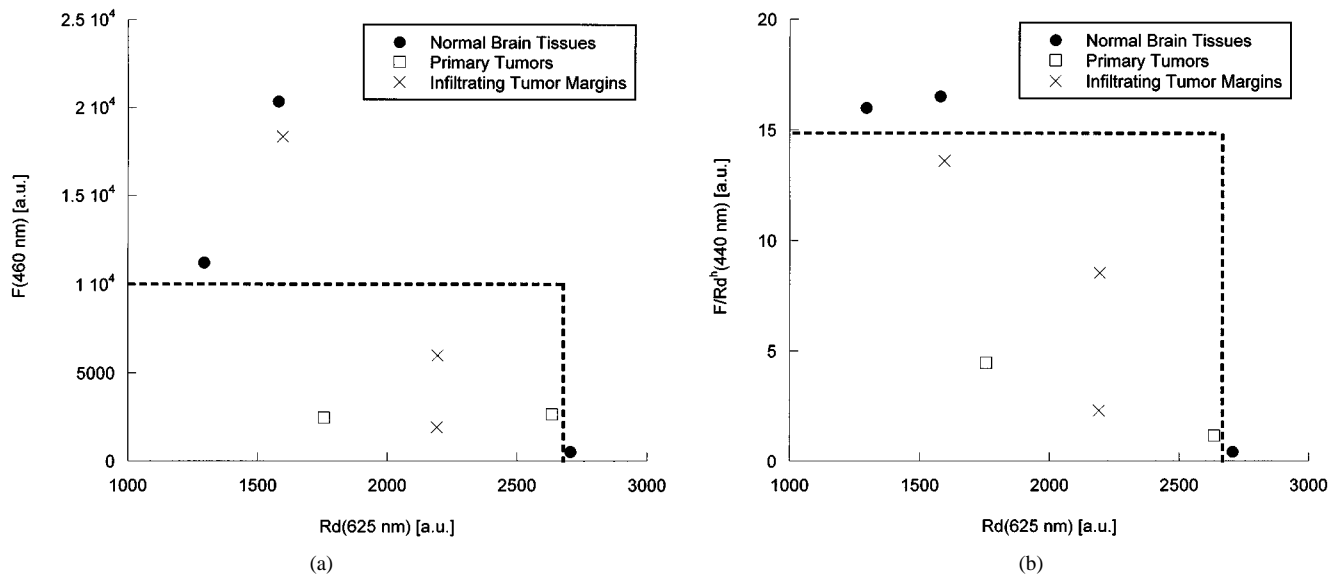


Fig. 5. Empirical discrimination algorithms for *in vivo* brain tissue data set with a high degree of superficial blood contamination based on: (a) $F(460 \text{ nm})$ and $Rd(625 \text{ nm})$ and (b) $F/Rd^{1.01}$ at 440 nm and $Rd(625 \text{ nm})$. Dashed line: cutoff for brain tissue separation.

of oxyhemoglobin. This assumption is found to be valid only between 300 and 600 (see Fig. 1). The significant differences between $h_{\text{dilute_blood}}$ and h_{oxyHb} beyond 600 nm indicate that $\mu_{a,\text{diluted_blood}}(\lambda_m)$ were over-estimated in this wavelength region. There is an increase in the amount of light scattering in the diluted blood solution between 600 and 800 nm which, leads to an additional loss of transmitted light energy. The transmission loss caused by scattering is treated as a loss caused by absorption when $\mu_{a,\text{diluted_blood}}(\lambda_m)$ are calculated based on transmission of the sample and Beer's Law. This limitation, however, should not prevent the applicability of the F/Rd^h model in most *in vivo* optical diagnostic applications that are based on autofluorescence spectroscopy, as tissue fluorescence is primarily observed between 400 and 600 nm.

Both the theory and the Monte Carlo simulation model (Fig. 2) suggest that F/Rd^h should be independent of the

degree of superficial blood contamination. However, the experimental results do not fully support this statement; F/Rd^h significantly deviates from theoretical predictions when α_f exceeds 2. This deviation may be attributed to the poor signal to noise ratio of F_c at high α_f , which may be improved by using a longer integration time and/or a higher excitation power. Nevertheless, the F/Rd^h model remains effective for $\alpha_f < 2$, which corresponds to a fluorescence attenuation of approximately 86%. Based on observations made during clinical spectroscopic studies in the brain, fluorescence signal attenuation encountered *in vivo* is typically less than 70%. This implies that the F/Rd^h model is definitely useful in a clinical situation (e.g., brain tumor resection).

The advantage of using F/Rd^h for *in vivo* tissue differentiation is clearly demonstrated in Figs. 4 and 5. Note that $Rd(625 \text{ nm})$, used in both discrimination algorithms, is

essentially free of any spectral attenuation due to superficial blood contamination since blood absorption is rather insignificant beyond 620 nm. While the best empirical discrimination algorithm based on raw spectral data (i.e., F (460 nm) and/or Rd (625 nm)) failed to completely separate normal brain tissues from tumor-bearing brain tissues in the case where the superficial blood contamination effect is pronounced, the optimal discrimination algorithm based on F/Rd^h ($h = 1.01$) at 440 nm and Rd (625 nm) yields a perfect separation. This clearly demonstrates the advantage of using F/Rd^h for *in vivo* brain tissue discrimination and the importance of removing the attenuation effect of superficial blood contamination in order to achieve accurate *in vivo* tissue differentiation using optical spectroscopy.

It should be emphasized that the theoretical basis of the spectral processing algorithm proposed in this paper, the F/Rd^h model, is a simple but distinct model that is meant to only account for the attenuation effect of a superficial blood layer typically present on the tissue surface in an operating field. The development of this algorithm was driven by the fact that the superficial blood layer seen particularly during surgical procedures is variable and is not intrinsic to the tissue. Hence, minimizing its influence on the tissue optical spectra is critical for the successful application of optical spectroscopy for intraoperative use and surgical guidance (as indicated in Fig. 5). Despite the fact that it does not remove the interplay of tissue optics in the fluorescence spectra [3]–[8], the F/Rd^h model significantly the performance of optical spectroscopy for *in vivo* brain tissue differentiation, as illustrated in Figs. 4 and 5. This spectral processing algorithm will be applied to the entire clinical data acquired from brain tumor patients *in vivo* and the impact of F/Rd^h on tissue discrimination will be thoroughly analyzed. The results of this part of study will be presented in the near future.

VI. CONCLUSION

The theory presented in this paper shows that combined optical spectroscopy F_c/Rd_c^h reduces the effect of superficial blood contamination present at the tissue surface, and hence removes one of the major obstacles toward the application of optical spectroscopy for intraoperative use and surgical guidance. This theory has been validated in a simulation as well as experimentally. It should be noted that the exponents $h(\lambda)$ between 300 and 600 nm can be predetermined using the absorption spectrum of oxyhemoglobin. Hence, the combined optical spectrum F_c/Rd_c^h , instead of the fluorescence spectrum F_c , should be used in the development of *in vivo* tissue discrimination algorithms for detection of disease.

REFERENCES

- [1] N. Ramanujam, "Fluorescence spectroscopy of neoplastic and nonneoplastic tissues," *Neoplasia*, vol. 2, pp. 89–117, 2000.
- [2] R. Richards-Kortum and E. Sevick-Muraca, "Quantitative optical spectroscopy for tissue diagnosis," *Ann. Rev. Phys. Chem.*, vol. 47, pp. 555–606, 1996.
- [3] J. Wu, M. Feld, and R. Rava, "Analytical model for extracting intrinsic fluorescence in turbid media," *Appl. Opt.*, vol. 32, pp. 3585–3595, 1993.
- [4] A. Durkin, S. Jaikumar, N. Ramanujam, and R. Richard-Kortum, "Relationship between fluorescence spectra of dilute and turbid samples," *Appl. Opt.*, vol. 333, pp. 414–423, 1994.
- [5] G. Gardner, S. Jacques, and A. Welch, "Fluorescence spectroscopy of tissue: Recovery of intrinsic fluorescence from measured fluorescence," *Appl. Optics.*, vol. 35, pp. 1780–1792, 1996.
- [6] R. Alfano and N. Zhadin, "Correction of the internal absorption effect in fluorescence emission and excitation spectra from absorbing and highly scattering media; theory and experiment," *J Biomed Optics*, vol. 3, pp. 171–186, 1998.
- [7] B. Pogue and G. Burke, "Fiber-optic bundle design for quantitative fluorescence measurement from tissue," *Appl. Opt.*, vol. 37, pp. 7429–7436, 1998.
- [8] Q. Zhang, M. Muller, J. Wu, and M. Feld, "Turbidity-free fluorescence spectroscopy of biological tissue," *Opt. Lett.*, vol. 25, pp. 1451–1453, 2000.
- [9] J. Folkman, "Tumor angiogenesis," in *The Molecular Basis of Cancer*, J. Mendelsohn, P. Howley, M. Israel, and L. Liotta, Eds. Philadelphia, PA: Saunders, 1995.
- [10] D. Hawrysz and E. Sevick-Muraca, "Developments toward diagnostic breast cancer imaging using near-infrared optical measurements and fluorescent contrast agents," *Neoplasia*, vol. 2, pp. 388–417, 2000.
- [11] F. Koenig, R. Larnie, H. Enquist, F. McGovern, K. Schomacker, N. Kollias, and T. Deutsch, "Spectroscopic measurement of diffuse reflectance for enhanced detection of bladder carcinoma," *Urology*, pp. 342–345, 1998.
- [12] W. Stummer, S. Stocker, S. Wagner, H. Stepp, C. Fritsch, C. Goetz, A. E. Goetz, R. Kiefmann, and H. J. Reulen, "Intraoperative detection of malignant gliomas by 5-aminolevulinic acid-induced porphyrin fluorescence," *Neurosurgery*, vol. 42, pp. 518–25, 1998.
- [13] E. Sebern, C. Brennan, and I. Hunter, "Design and characterization of a laser-based instrument with spectroscopic feedback control for treatment of vascular lesions: The "Smart Scalpel"," *J. Biomed. Opt.*, vol. 5, pp. 375–382, 2000.
- [14] A. Morguet, R. Gabriel, A. Buchwald, G. Werner, R. Nyga, and H. Kreuzer, "Single-laser approach for fluorescence guidance of excimer laser angioplasty at 308 nm: Evaluation in vitro and during coronary angioplasty," *Lasers Surg. Med.*, vol. 20, pp. 382–393, 1997.
- [15] S. Boppart, J. Herrmann, C. Pitris, D. Stamper, M. Brezinski, and J. Fujimoto, "High-resolution optical coherence tomography-guided laser ablation of surgical tissue," *J. Surg. Res.*, vol. 82, pp. 275–284, 1999.
- [16] W.-C. Lin, S. A. Toms, M. Johnson, E. D. Jansen, and A. Mahadevan-Jansen, "In vivo brain tumor demarcation using optical spectroscopy," *Photochem. Photobiol.*, vol. 73, pp. 396–402, 2001.
- [17] S. A. Prahl. (1999) Optical Absorption of Hemoglobin. [Online]. Available: <http://omlc.ogi.edu/spectra/hemoglobin/index.html>
- [18] A. Welch, C. Gardner, R. Richards-Kortum, E. Chan, G. Criswell, J. Pfeifer, and S. Warren, "Propagation of fluorescence light," *Lasers Surg. Med.*, vol. 21, pp. 166–178, 1997.
- [19] W.-F. Cheong, "Summary of optical properties," in *Optical-Thermal Response of Laser-Irradiated Tissue*, A. Welch and M. J. van Gemert, Eds. New York: Plenum, 1995, pp. 275–301.
- [20] S. A. Prahl. (1999) Inverse Adding Doubling Program. [Online]. Available: <http://omlc.ogi.edu/software/iad/index.html>



Wei-Chiang Lin received the B.S. degree from Chung-Yung Christian University, Chung-Li, Taiwan, in 1985, and the M.S. and Ph.D. degrees from the University of Texas at Austin, Austin, TX, in 1994 and 1997, respectively, all in biomedical engineering.

He is currently a Research Assistant Professor of Biomedical Engineering at Vanderbilt University, Nashville, TN. His research interests include optical spectroscopy, tissue optics, and tissue mechanical properties. He is involved in the development of

optical spectroscopic based systems for surgical guidance.



Steven A. Toms received the M.D. degree from Brown University, Providence, RI, in 1989, and the M.P.H. degree from the School of Public Health and Hygiene, The Johns Hopkins University, Baltimore, MD, in 1992.

He completed his residency training in preventive medicine at The Johns Hopkins University Hospital and in neurological surgery at the Cleveland Clinic Foundation in 1992 and 1998, respectively. Until recently, he was an Assistant Professor of Neurological Surgery and Otolaryngology at Vanderbilt University Medical Center. He is currently with Oregon Health Sciences University, Portland. His clinical expertise is in neuro-oncology and his research interests are in the area of therapeutics and diagnostics for glioblastoma multiforme.



Anita Mahadevan-Jansen received the B.S. and M.S. degrees in physics from the University of Bombay, Bombay, India, in 1988 and 1990, respectively, and the M.S. and Ph.D. degrees in biomedical engineering from the University of Texas at Austin in 1993 and 1996, respectively.

He joined the faculty of the Department of Biomedical Engineering at Vanderbilt University, Nashville, TN, in the fall of 1998. Her expertise is in the area of optical spectroscopy and imaging, specifically on the application of fluorescence and Raman spectroscopy for the detection of tissue physiology, as well as pathologies such as cancers.



E. Duco Jansen received the M.S. degree in medical biology from Utrecht University, The Netherlands, in 1990, and the M.S. and Ph.D. degrees in biomedical engineering from the University of Texas at Austin, in 1992 and 1994, respectively.

He joined the faculty of the Department of Biomedical Engineering at Vanderbilt University as Assistant Professor in 1997. His research interests are in therapeutic applications of lasers and novel, noninvasive methods of optical imaging of biological tissues.